



Experimental Investigation of Tool Lifespan Evolution During Turning Operation Based on the New Spectral Indicator OL_{mod}

Mohamed Khemissi Babouri^{1,2} · Nouredine Ouelaa¹ · Mohamed Cherif Djamaa¹ · Zakarya Ouelaa¹ · Lilia Chaabi³ · Abderrazek Djebala¹

Received: 28 April 2023 / Revised: 6 September 2023 / Accepted: 6 October 2023 / Published online: 1 November 2023
© Springer Nature Singapore Pte Ltd. 2023

Abstract

Purpose The cutting tool wear is one of the major physical phenomena to be studied in order to optimize the production and to guarantee the quality of manufactured products. Indeed, the wear affects the quality of the machined surfaces, the durability of the cutting tool and the imposed geometric tolerances. Since uncontrolled wear can lead to premature tool breaking and therefore a drop in productivity, monitoring the machining process is a necessary important task.

Methods In this study, aims to combine experimental results from vibration signature and cutting forces with experimental and numerical methodology allowing the prediction of optimal lifetime of the tool's wear, and to detect the brutal damage of this last, based especially an optimized wavelet multi-resolution analysis (OWMRA), allowed the denoising of the measured signals.

Results The OWMRA revealed two peaks, which appear below and above the tool's resonance frequency. The amplitude evolution of these two peaks is directly related to the effect of the tool wear on the natural frequency band. The strategy adopted is based on a slight modification of a new spectral indicator and in particular the modified overall level (OL_{mod}) calculated from the cutting forces and reconstructed signals.

Conclusions The modified overall level (OL_{mod}) has also shown its effectiveness of providing the moment of transition of the wear of its normal phase to accelerated phase around the band of the cutting tool characteristic frequencies, corresponding to catastrophic wear leading to stopping machining at the appropriate time and which can alert the user as soon as the criterion of the transition to catastrophic wear is reached.

Keywords Tool wear monitoring · Tool lifespan · Modified overall level · Wavelet multi-resolution analysis

Abbreviations

A_j	Approximations	D_j	Detail
AE	Acoustic emission	db5	Daubechies 5
a_p	Depth of cut, mm	DWT	Discrete wavelet transform
CWT	Continuous wavelets transform	EA	Envelope analysis
		EEMD	Ensemble empirical mode decomposition

✉ Mohamed Khemissi Babouri
babouri_bmk@yahoo.fr

Nouredine Ouelaa
n_ouelaa@yahoo.fr

Mohamed Cherif Djamaa
djamaa.mohamedcherif@univ-guelma.dz

Zakarya Ouelaa
z_ouelaa@yahoo.com

Lilia Chaabi
lilia_chaabi@yahoo.fr

Abderrazek Djebala
djebala_abderrazek@yahoo.fr

¹ Mechanics and Structures Laboratory (LMS), University 8 May 1945 Guelma, Po. Box 401, 24000 Guelma, Algeria

² Department of Mechanical Engineering and Productics (CMP), FGM & GP, University of Sciences and Technology Houari Boumediene, El-Alia, Bab-Ezzouar, Po. Box 32, 16111 Algiers, Algeria

³ Laboratory of Electrical Engineering of Guelma (LGEG), University 8 May 1945 Guelma, Po. Box 401, 24000 Guelma, Algeria

f	Feed rate, mm/rev
F_y	Radial cutting force, N
ICEEMDAN	Improved complete ensemble empirical mode decomposition with adaptive noise
Kur	Kurtosis
KT	Crater wear, mm
OL_{mod}	Overall level
OWMRA	Optimized wavelet multi-resolution analysis
RMS	Root mean square
R_a	Arithmetic mean roughness, μm
R_t	Total roughness, μm
R_z	Mean depth of roughness, μm
$s(t)$	Signal
T	Cutting time, s
TCMS	Tool condition monitoring systems
VB	Flank wear, mm
V_c	Cutting speed, m/min
MW	Mother wavelet
WT	Wavelet transform

Introduction

The monitoring of cutting tool's wear has great significance and becomes a priority in the advanced machining processes, with the aim of increasing productivity while guaranteeing the quality of machined surfaces and the required geometric tolerance. Tools wear results from severe thermal and mechanical stresses that the cutting edge undergoes. Moreover, the machining process is often faced with vibrations, which have negative influence on the surface quality of the work-piece, and cause premature cutting tool wear.

In this context, the tool's wear monitoring in advanced machining processes requires the implementation of an effective follow-up system based on the processing of measured signals from which some indicators directly related to the wear evolution can be extracted. However, wear is very complex to monitor during the different phases of the cutting process since the measured signals are often affected by the material nature of the work-piece, the geometry and the material of the cutting tool, and the cutting conditions. Indeed, several recent techniques have been proposed to monitor in continuous the tool wear, which are based on the analysis of different measurements; cutting forces, acoustic emission, vibration signals, etc. [1]. Other physical quantities have been used in various tool condition monitoring systems [2, 3] that based on the measurement of stresses and strains as in the work of Zhou et al. [4] to monitor the stresses acting on the tool cutting edge during the machining process to predict sudden tool breaking. Li et al. [5] concluded that it was possible to predict the cutting tool breaking through measurements of electric current and motor

power, while Oo HtunHtun et al. [6] used image processing techniques for tool wear monitoring.

Recently, many works have been developed especially with regard to the monitoring of cutting tool's wear, which affects the vibration signals taken during machining. In the work of Zhou et al. [7] chose holder exponents to estimate the vibration signals singularity of the milling tool. A method of selecting the optimal wavelet bases is used to identify the transition point of the tool wear. Navarro-Devia et al. [8] have shown that high frequency vibrations can occur in the three directions with different amplitudes, which are located near the natural frequencies. In a recent study, Huang et al. [9], to expose the influence of the tool wear on the cutting force and spindle acceleration signals, performed several experiments. The results analysis concluded that the cutting force (F_y) obviously increases with the increase in tool wear compared to the two other directions (F_x and F_z). In [10], the authors proposed a study to demonstrate the impact of the tool wear on the vibration amplitudes affecting the machining system. Chiou and Liang [11] investigated and evaluated the effect of flank tool wear on chatter RMS acoustic emission (AE) signals through a dynamic model; they found that the chatter vibration amplitude is around the chatter frequency of the cutting tool. In the same context, Zhu and Zhang [12] developed a generic explicit wear model based on adjustable coefficients. The obtained results show a high on-line predicted accuracy of the tool lifespan and the instantaneous force modeling with wear model.

Extracting significant information on tool failure from the measured signals is possible through preprocessing techniques via different domains [13]; time domain [14, 15] and frequency domain [16, 17]. However, the frequency domain is preferred to choose the optimal frequency band, sensitive to the tool wear. Therefore, an ideal approach based on time–frequency analysis [18, 19] is employed to extract the right frequency band.

Recent works [20, 21] have shown that mask effects, in particular random noise and other machine components signals, pollute the measured signals and make the tool wear monitoring difficult. To avoid this problem, filtering and denoising methods have been developed to provide feature extraction of the wear signature from the original measured signal. In the work of Babouri et al. [22], the authors proposed the empirical mode decomposition (EMD) to improve the sensitivity of the energy (E) and the mean power (P_{moy}), as two scalar indicators, to the wear variation. The main originality of this work is undoubtedly the use of a new indicator; the amplitude of the peak corresponding to the natural frequency of the optimal reconstructed signal (IMF1) obtained by the EMD. The results show that it is more preferable to take the variation of this frequency indicator over the entire cutting tool life allowing the detection of the critical transition point that indicates the start of the catastrophic

wear phase of the cutting tools. In [23], the EEMD was combined with a support vector machine to estimate milling tool wear. In [24], the spectral kurtosis analysis applied to the vibration signals allows to locate the frequency band and the empirical decomposition with ICEEMDAN is used to isolate the significant optimal vibration modes. The energy of high-frequency vibration modes that can be used for tool wear monitoring has been observed.

The work presented in this paper consists in using an experimental and numerical approaches based on an Optimized Wavelet Multi-Resolution Analysis to find the correlation between tool wear and time–frequency indicators.

The article is structured as follows. In section "Theoretical foundations and lifespan monitoring method", presents the theoretical and mathematical foundations of the analysis methods, in particular OWMRA. Section "Experimental setup" includes a detailed presentation of the experimental procedure and the methodology proposed to perform the various experimental measurements. Section "Vibratory responses and wear study" presents the analysis of vibration responses for wear monitoring and their evolution. Section "Prediction of the tool lifespan" is devoted to the discussion of the results obtained, and the study of the application of a new spectrum indicator called the Modified Overall Level (OL_{mod}), which is calculated from the cutting forces and reconstructed signals for prediction of the tool lifespan around the band of the cutting tool characteristic frequencies. Finally, a conclusion is given in Section "Conclusion".

Theoretical Foundations and Lifespan Monitoring Method

Optimized Wavelet Multi-resolution Analysis

The wavelet transform (WT) replaces the sinusoids of the Fourier Transform by a family of translations and dilations of the same function called wavelet. A mother wavelet ψ is a basic function that can translate and dilated over the time–frequency domain to analyze the signal. The wavelet

must be a function of zero mean; in other words, ψ must be a wave.

$$\int_{-\infty}^{+\infty} \psi(t)dt = 0. \tag{1}$$

The translation b and scale (or dilation) a factors are then introduced. Mathematically, the wavelet family is put in the form [21, 25]:

$$\psi_{a,b}(t) = \frac{1}{\sqrt{a}}\psi\left(\frac{t-b}{a}\right). \tag{2}$$

Noting ψ^* the conjugate of ψ , the wavelet transform of a function $s(t)$ is defined by:

$$CWT = \frac{1}{\sqrt{a}} \int_{-\infty}^{+\infty} s(t)\psi^*\left(\frac{t-b}{a}\right)dt. \tag{3}$$

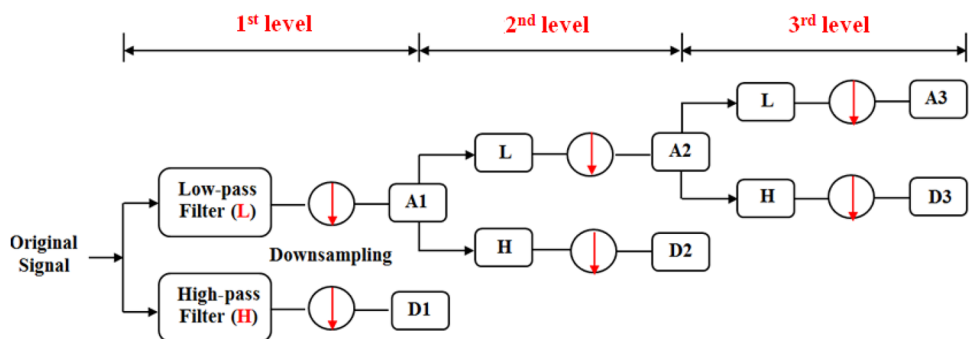
This transform is assumed continuous, denoted CWT (Continuous Wavelet Transform). The discrete wavelet transform (DWT) is a discretization of the continuous wavelet transform. By replacing a and b by 2^m and $n2^m$, respectively, its expression becomes:

$$DWT = 2^{-\frac{m}{2}} \int_{-\infty}^{+\infty} s(t)\psi^*(2^{-m}t - n)dt, \tag{4}$$

with m and n integers.

Wavelets are used to represent a signal in time–frequency domain because they allow better localization than Fourier Transform. The decomposition is done from a set of basic wavelets obtained from a mother wavelet $\psi(x)$. This transformation describes the details of a signal for each level of resolution. These details correspond to the difference in information between two successive resolution levels. To this end, Mallat [26] had the idea of considering the wavelet analysis as a waterfall decomposition of the signal $s(t)$ associating a pair of filters at each level of resolution, low-pass filters (L) and high pass (H). At this level, two vectors will

Fig. 1 Principle of the waterfall decomposition at 3 levels



be obtained: cA1 and cD1, called approximation and detail coefficients, respectively. This version of wavelet analysis is called Wavelet Multi-resolution Analysis (WMRA).

The decomposition procedure can be repeated several times with the approximation coefficient cA1 and for each new vector cAk obtained. Figure 1 represents the wavelet decomposition of a signal $s(t)$ for three levels using Mallat’s algorithm. During decomposition, the measured signal $s(t)$ and the approximation coefficients (cAk) undergo subsampling and this is the reason why the cAk and cDk vectors pass again through two reconstruction filters (LR) and (HR). Two vectors will be obtained: the Ak vectors are called the approximations, which correspond to the lower frequencies, while the Dk vectors are called the details, which correspond to the higher frequencies, satisfying the following relation:

$$A_{j-1} = A_j + D_j$$

$$s = A_j + \sum_{i \leq j} D_i, \tag{5}$$

where i and j are integers.

Therefore, each wavelet has its own filters bank, which allows the multiresolution analysis. Several signals of different frequency bands will then be obtained, called details (D_j) and approximations (A_j). The WMRA is widely used in the processing of measured signals in several laboratory and industrial applications, in particular for filtering and denoising the measured signals on rotating machines to detect potential mechanical defects.

An optimized version of the WMRA (Fig. 2), especially adapted for the analysis of shock signals, was proposed by Djebala et al. [27, 28]. Using the kurtosis as a main criterion, several parameters were selected: the type of the mother wavelet, the sampling frequency, the optimal vector, the number of levels, etc. This optimized version was

successfully applied for the detection of rolling bearing and gear defects. It was noticed that the application of Optimized WMRA on vibration signals is essentially affected by four rational choices of the major analysis parameters:

- The choice of the optimal measurement parameters of the monitoring system;
- The choice of a family of optimal mother wavelets;
- The choice of the optimal number of WMRA levels;
- The choice of the optimal vector of the wavelet decomposition;

The principal measurement parameters are the sampling rate, the rotation speed ranges and the maximum frequency. Consequently, the maximum frequency of the final level approximation $F_{max}(A_n)$ must imperatively be three times equal to the shock frequency F_c to confirm the defect frequency existence [27], which gives by:

$$F_{max}(A_n) = \frac{F_{max(x)}}{2^n} = 3F_c. \tag{6}$$

So, the number of levels must satisfy:

$$n = 1.44 \log \left(\frac{F_{max(x)}}{3F_c} \right). \tag{7}$$

In our case, the optimal vector of the wavelet decomposition is the one, which allows the defect detection with the best possible resolution, and leads to select the best filtered one with the largest kurtosis.

The main contribution of this paper is to adapt the optimized WMRA for the analysis of cutting forces signals measured during the machining process. The obtained results can give accurate prediction of the cutting tool wear before its total failure. The cutting process signals

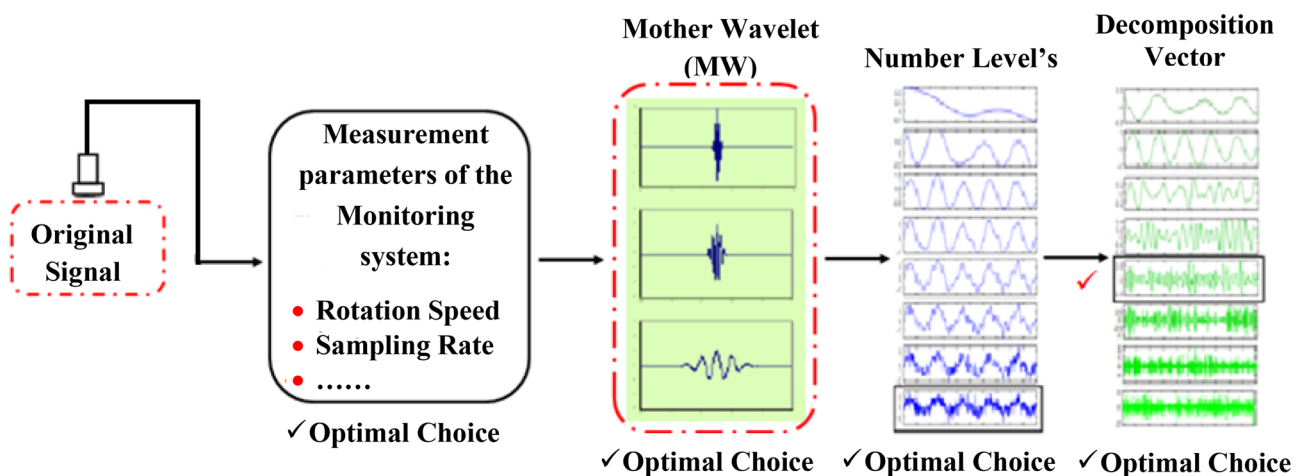


Fig. 2 The OWMRA process

are generally non-stationary due to the non-linearity of the cutting process outputs and the non-homogeneity of the work-piece. In practice, the variation of the cutting force can be correlated with the tool wear since it increases considerably with the increase in the wear band.

Frequency Indicators

Frequency indicators are those calculated from the spectra as given by the analyzer or after the application of the Fourier transform. Among these indicators, we can mention the overall level OL. To make this indicator more effective in detecting changes in the wear value of cutting tools, Babouri and Ouelaa [25] proposed a slight modification on the expression of the overall level (OL_{mod}) by limiting the calculation to the sum of the number of lines of the spectrum around the resonant frequency of the cutting tool, delimited by F_{max} and F_{min} frequencies. The expression of the overall level OL_{mod} is given by:

$$OL_{mod} = \sqrt{\frac{2}{3} \sum_{F_{min}}^{F_{max}} (N_i)^2}, \tag{8}$$

with N_i the number of lines of the spectrum in the same band.

Cutting Tool Lifespan Monitoring

Generally, the flank wear (VB) is considered as the most used criterion to evaluate the cutting tool life [29–31]. Theoretically and also in practice, the evolution of flank wear as a function of machining time passes through three phases as

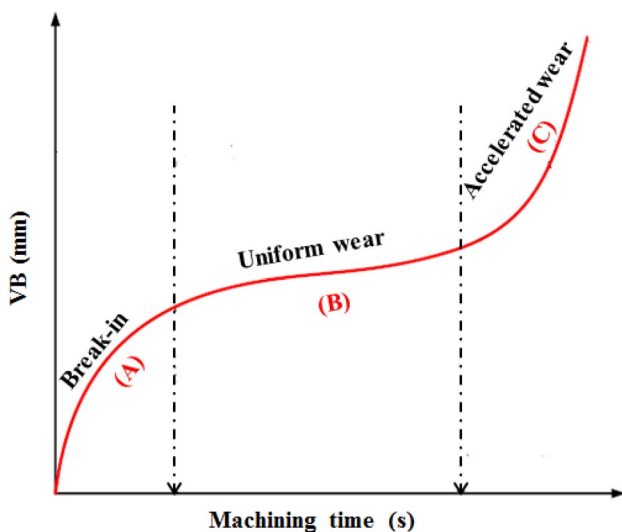


Fig. 3 Theoretical tool wear

illustrated in Fig. 3: initial wear phase (A), wear stabilization (B) and accelerated wear (C).

The cutting tool lifespan is characterized by the productive time during which the cutting edge retains its cutting power that directly depends on its degree of wear. When the wear reaches a certain critical value, the cutting forces, the temperature and the vibrations increase significantly and deteriorate the stability of the cutting process. Thus, the latter influences productivity, the machined workpiece quality and the machining cost. Hence the interest of predicting the cutting tool life during machining before its almost complete degradation. The monitoring approach was reached as shown in the flowchart in Fig. 4.

In this context, the monitoring device of a cutting tool wear must allow the sampling of a signal and its processing to allow the detection of an excessive wear. Note that the measured signals among the cutting process are generally non-stationary due to the non-linearity of the cutting process and the non-homogeneity of the workpiece. To this end, the right choice of measuring data and the processing device is essential for online monitoring. This process depends on the sensor and the signal quality to extract the useful

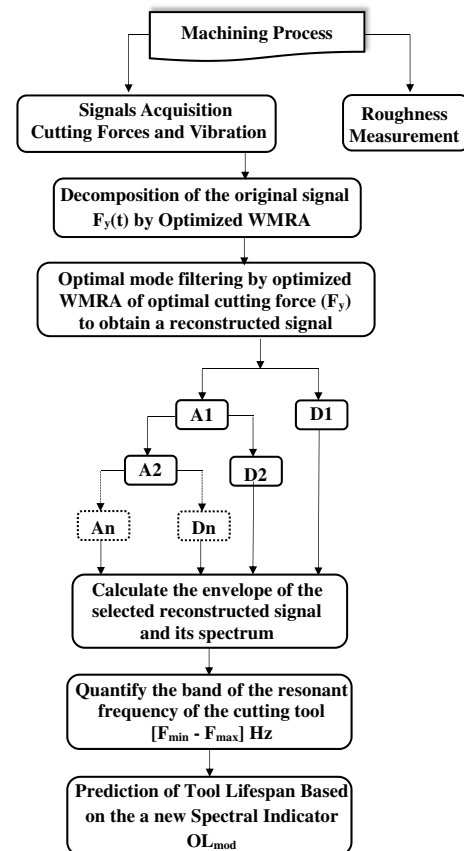


Fig. 4 The flowchart of the proposed approach

information embedded in these signals either by analysis or by filtering.

The present investigation aims to determine the relationship between cutting forces and vibrations associated with the cutting tool's wear. It aims also to evaluate the possibility of the prediction of the tool's lifespan by means of a new proposed spectral indicator and to show its effectiveness to determine the moment of transition of wear from its normal phase to the accelerated phase, corresponding to catastrophic wear.

Experimental Setup

Experimental Conditions

The machining operations were performed on a SN40C lathe with a spindle power of 6.6 kW. The machined steel in the experiments is X200Cr12, which has excellent wear resistance. It is mainly used for the manufacture of cutting tools body, punches tools, measuring instrument. Its chemical composition is given as follows: 11.50% Cr; 2% C; 0.30% Mn; 0.70% W and 0.25% Si. The mechanical and physical characteristics of this steel are as follows: thermal conductivity 20 W/mC°; density 7.7 kg/m³ and elasticity modulus of 21.10 MPa. For all the tests, round bars with a diameter of 62 mm and a length of 480 mm are used. Square inserts of uncoated carbide S40T are used, their composition is: 11.0% Co, mixed carbides 12.0% and CW remainder, grain size is 1–2 μm and their hardness HV 1420. The insert is mounted on a tool holder CSBNR 2525 M12, the geometry of the active part of the tool is described as follows: $\alpha=6^\circ$; $\chi=75^\circ$; $\lambda=-6^\circ$ and $\gamma=-6^\circ$ [32]. The machining tests were carried out without lubrication and under the following cutting conditions: $V_c=100$ m/min, 135 m/min and 190 m/min, $a_p=0.5$ and 1 mm, and $f=0.12$ mm/rev.

Data Acquisition and Measurement Setup

The cutting force signals generated during machining were acquired using a KISTLER dynamometer (model 9257B), which allows to measure the intensity of the cutting forces in real time in the three main cutting directions with a sampling rate of 10.800 kHz. On the other hand, acceleration signals are measured using a B&K 2035 two-channel signal analyzer, with two piezoelectric accelerometers B&K 4384 type placed on the cutting tool in both tangential and radial directions for a sampling frequency of 32.768 kHz. After each experiment, the tool was cleaned to remove steel residuals and new cutting edge was used. For the measurement of the flank wear (VB) and the crater wear (KT), an optical microscope HUND type WAD and a comparator equipped with a sharp tip probe following the profile of the crater are used, respectively. At the end of each test, roughness measurements were performed on the machining surfaces to analyze the effect of the different cutting parameters using a roughness meter “Surftest 301 Mitutoyo”. Figure 5 shows the schematic diagram relating to the experimental procedure for the wear measurement and data acquisition system. The technical characteristics of the test bench components are summarized in Table 1.

Using the experimental setup, illustrated by Fig. 6, some series of tests was performed for different combinations of cutting conditions. During each test, both signals of two acceleration components and three cutting force components are recorded. At the end of each test, the measurement of VB and KT wear as soon as the Ra roughness are done (Table 2) The processing of the collected signals was established using an analysis software developed under MATLAB environment.

Fig. 5 General view of the signal acquisition setup

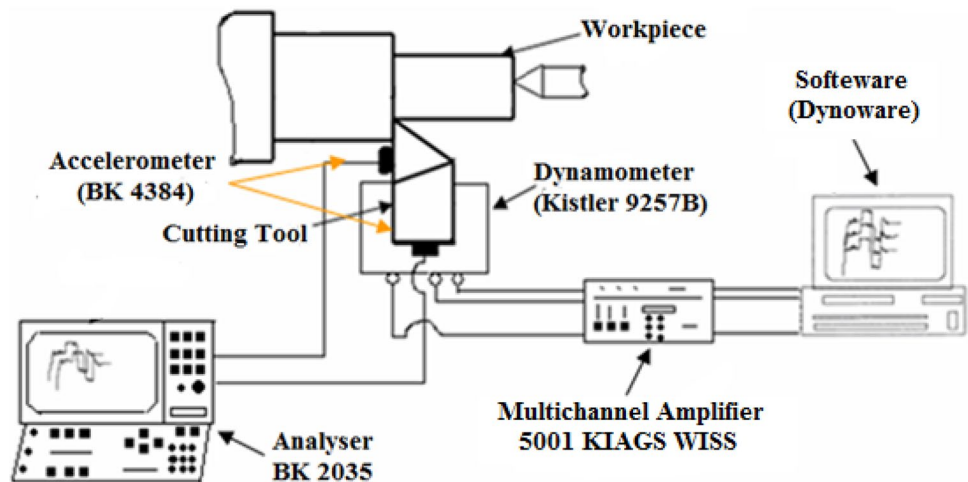


Table 1 Experimental results for X200Cr12

Runs	Machining time (s) t	Flank wear (mm) VB	Crater wear (mm) KT	Roughness (μm)		
				R_a	R_t	R_z
(a) $V_c = 100$ m/min, $a_p = 0.5$ mm, $f = 0.12$ mm/rev						
1	50	0.086	0.012	0.50	2.50	2.00
2	100	0.131	0.020	0.70	4.20	3.10
3	150	0.200	0.024	1.30	6.70	5.10
4	200	0.225	0.031	1.32	7.00	5.20
5	250	0.261	0.041	1.34	8.30	5.60
(b) $V_c = 135$ m/min, $a_p = 0.5$ mm, $f = 0.12$ mm/rev						
1	35	0.221	0.023	0.45	2.30	1.80
2	70	0.321	0.034	0.61	3.80	2.70
3	105	0.425	0.046	1.15	6.40	4.80
4	140	0.502	0.061	1.45	7.60	5.70
5	175	0.601	0.081	1.71	7.93	6.30
(c) $V_c = 190$ m/min, $a_p = 0.5$ mm, $f = 0.12$ mm/rev						
1	25	0.401	0.039	0.41	1.90	1.40
2	50	0.501	0.053	0.68	4.20	3.00
3	75	0.561	0.107	1.35	7.00	5.30
4	100	0.821	0.168	1.52	7.91	6.20
5	125	1.112	0.184	1.82	9.13	6.89
(d) $V_c = 100$ m/min, $a_p = 1$ mm, $f = 0.12$ mm/rev						
1	50	0.123	0.015	0.57	2.73	2.30
2	100	0.200	0.020	0.72	4.50	3.30
3	150	0.248	0.030	1.70	7.50	6.50
4	200	0.286	0.044	1.76	7.40	5.60
5	250	0.340	0.071	1.89	9.50	6.76
(e) $V_c = 135$ m/min, $a_p = 1$ mm, $f = 0.12$ mm/rev						
1	35	0.301	0.048	0.51	2.50	2.10
2	70	0.460	0.054	0.65	4.30	3.20
3	105	0.555	0.074	1.80	7.80	6.80
4	140	0.603	0.084	2.10	9.20	6.70
5	175	0.700	0.097	2.40	10.09	9.50
(f) $V_c = 190$ m/min, $a_p = 1$ mm, $f = 0.12$ mm/rev						
1	25	0.500	0.074	0.45	2.31	1.70
2	50	0.617	0.110	0.72	4.60	3.90
3	75	0.662	0.150	1.85	8.30	7.20
4	100	0.999	0.205	2.50	10.00	7.30
5	125	1.502	0.239	3.00	11.87	10.55

Experimental Modal Analysis

Before starting the experimental machining test, series of measurements was carried out to determine the natural frequencies of the cutting tool in horizontal and vertical directions using an instrumented shock hammer having a force sensitivity equal to 4 Pc/N (Fig. 7). The knowledge of the natural frequencies allows better analysis of the vibration and cutting force measurements, obtained subsequently.

In the horizontal direction (Fig. 8a), the results highlight the appearance of the first bending mode at 4000 Hz and the first torsion mode at 4776 Hz. Whereas in the vertical direction (Fig. 8b), the first torsion mode appears at 4760 Hz and the first bending mode appears at 5032 Hz. In both directions, appears the same torsion mode. The difference between the natural frequencies in the two directions is due to the difference of the tool rigidity in these two directions.

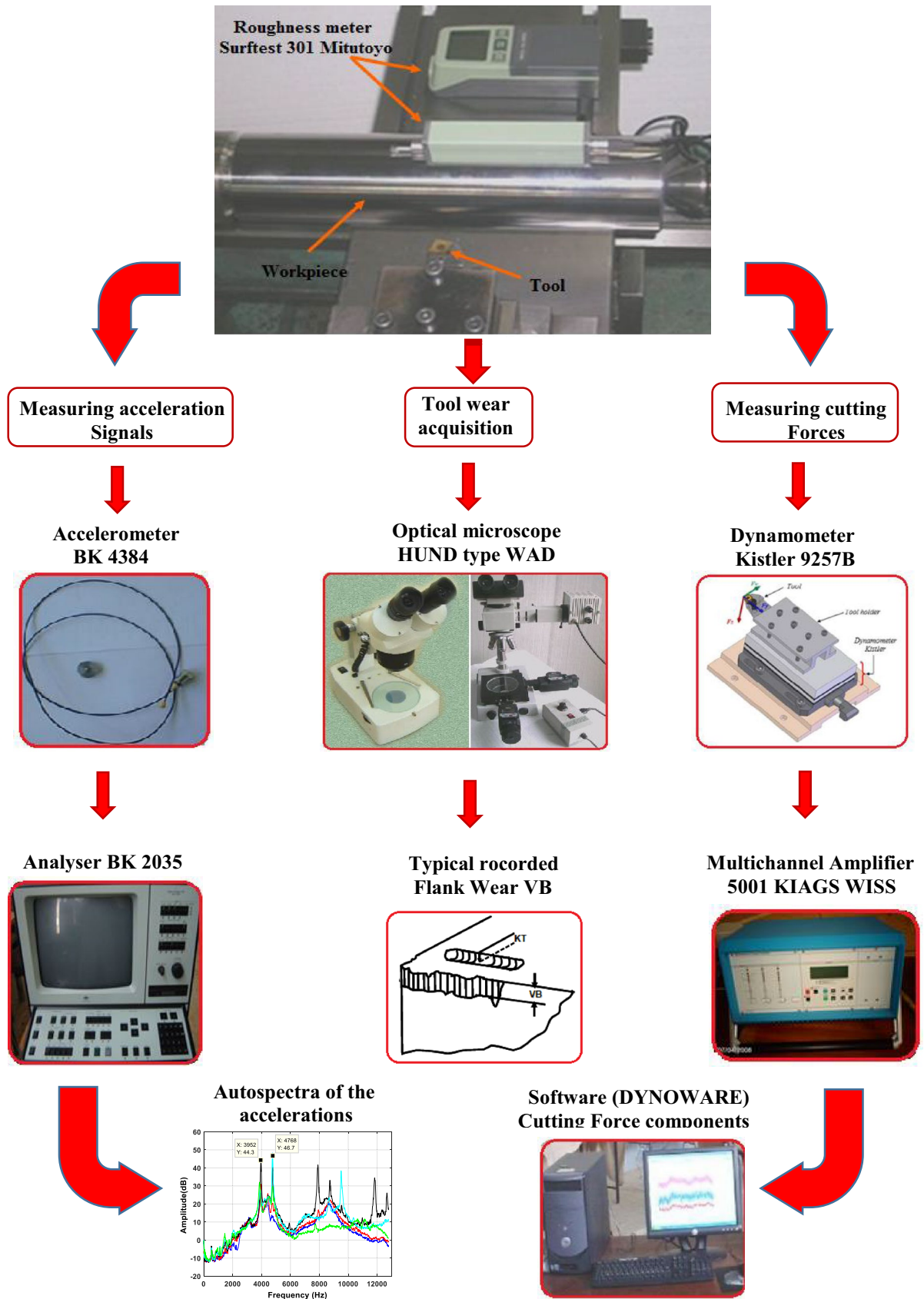
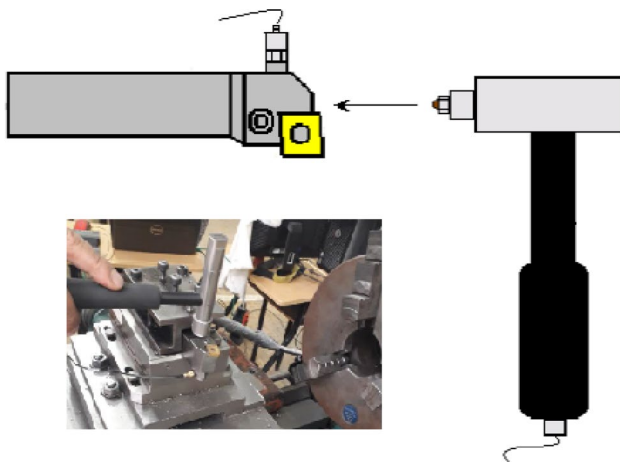


Fig. 6 Schematic diagram of the experimental setup and methodology

Table 2 Components of the test rig and the measurement material

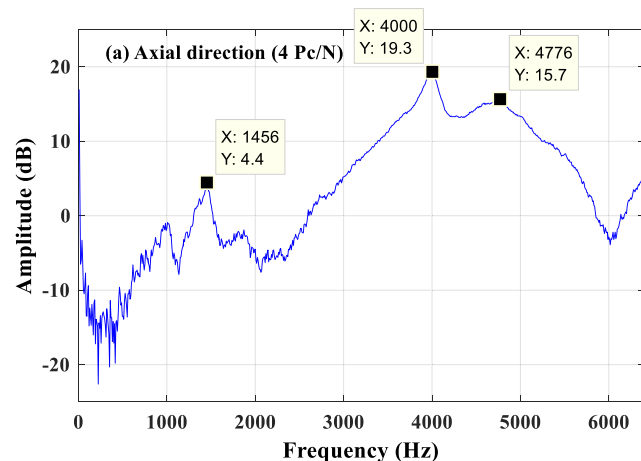
Components	Type	Technical characteristics
Piezoelectric accelerometer	Brüel & Kjaer 4384	Sensitivity: 0.99 PC/ms ⁻² Resonance frequency: 35 KHZ
Vibration analyzer	Brüel & Kjaer 2035	Frequency band: 0 to 25.6 kHz, Number of samples: 2048
Optical microscope	HUND type WAD	Precision: 0.001 mm
Roughness meter	Surfetest 301 Mitutoyo	0.05 to 40 μm for Ra, 0.3 to 160 μm for Rt and Rz, Tip radius of 5 μm
Amplifier	5001 KIAGS WISS	Multi channels; intended for measuring cutting forces
Dynamometer	Model 9257B	Four quartz sensors with three principal directions

**Fig. 7** Modal test of the cutting tool

Vibratory Responses and Wear Study

Vibration Signature for Wear Monitoring

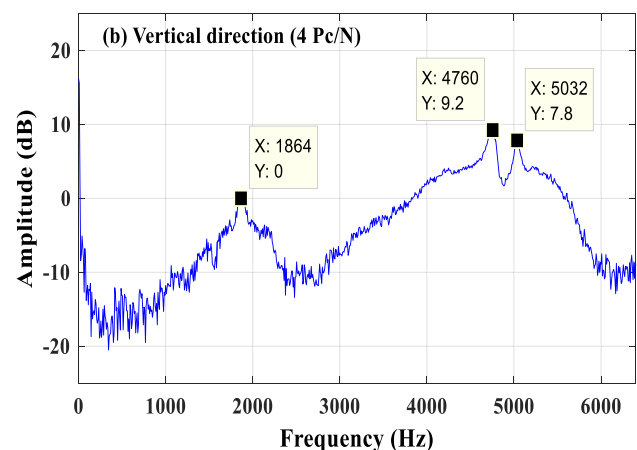
The signals are delivered by two accelerometers; the first one is placed on the support of the cutting tool in the longitudinal



direction and the second is placed at the tool free end in the vertical direction. For the entire machining interval, the autospectra are recorded from the first to the fifth sequences. The evolution of the acceleration autospectra as a function of the flank wear are shown in (Figs. 9 and 10).

The global analysis of the different autospectra shows that the phenomenon of wear appears on, below and/or above the natural frequencies of the cutting tool by an increasing of the background of the spectrum. For the longitudinal direction (Fig. 9), a decrease in the autospectra's magnitude as a function of the frequency is observed. Above the two first natural frequency peaks corresponding respectively to the bending and torsion modes, the level is below 0 dB for $VB \leq 0.3$ mm (Fig. 9a). For the other sequences where the wear exceeds 0.3 mm, the level reached approximately 15 dB, then it decreases following the importance of the wear, but in general remains greater than 0 dB (Figs. 9b and c).

However, the autospectra of the vertical direction (Fig. 10) show an inverse behavior to that of the longitudinal direction because other modes of the cutting tool appear at high frequencies. The level of the autospectra increases automatically but it is hard to relate it to wear. In the frequency band (0–2000 Hz), the level remains lower

**Fig. 8** Modal analysis of the system dynamometer-cutting tool

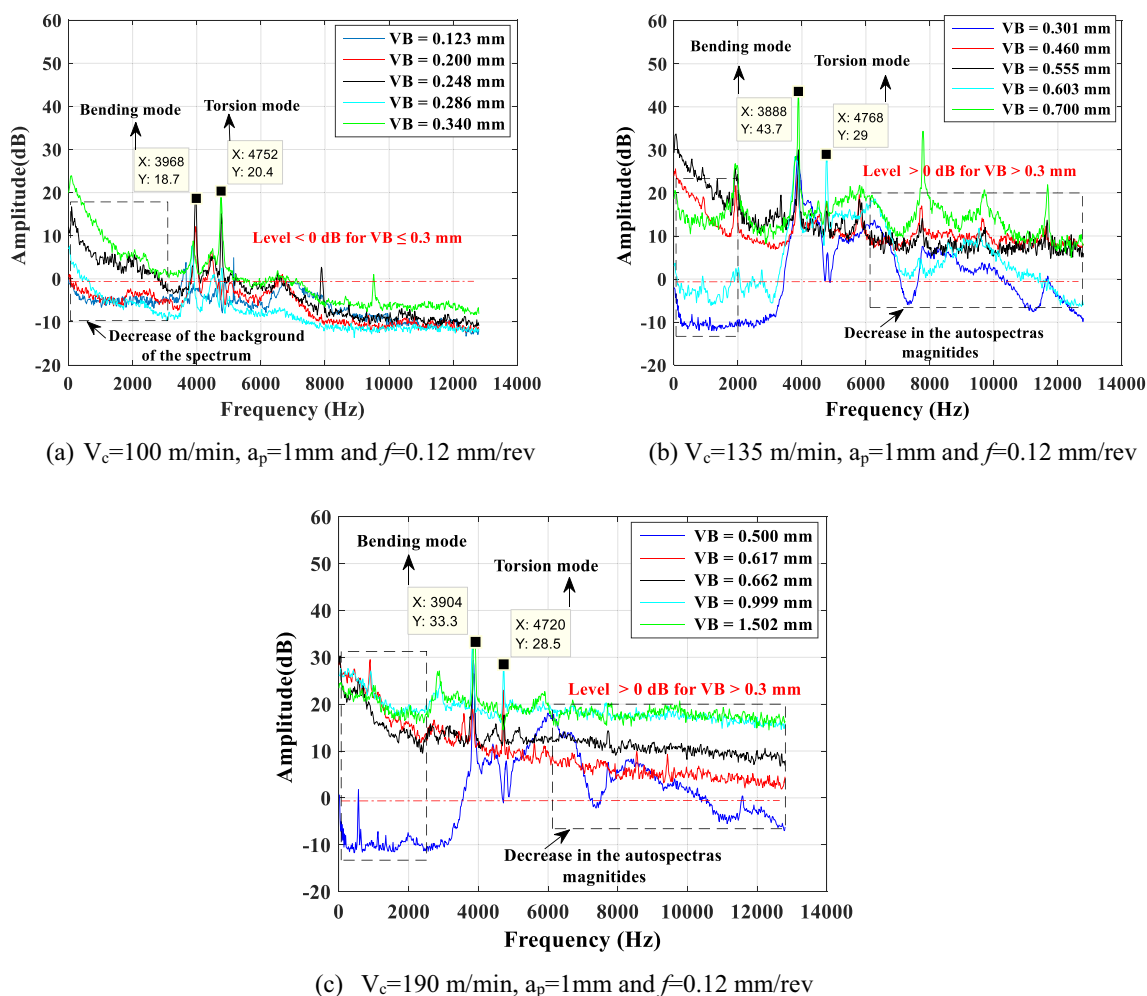


Fig. 9 The autospetra of accelerations in the radial direction for different sequences and with different flank wear (VB)

than 0 dB, but one note the appearance of a torsion mode peak starting from the fourth sequence, which corresponds to the end of the normal wear zone of the cutting tool (Fig. 10a).

In this context, for the two acceleration components, the amplitude variation of the peaks corresponding to the natural frequencies is not very affected by the increase in wear. In the vertical direction, one note the appearance of two peaks; the first is a bending mode of the cutting tool in the axial direction (3872 Hz) and the second linked to the torsion of the cutting tool (4720 Hz).

As a result, it is found that the energy of the autospetra of the acceleration signals does not exceed 0 dB except at resonance frequencies in the case where the flank wear does not exceed 0.3 mm. However, it considerably increases with the flank wear increase below the natural frequencies in the band (0–2) KHz, or above the band (6–12) KHz.

Evolution of Roughness and Flank Wear

The results of the roughness as a function of wear (Table 2) show that the increase in flank wear VB leads to a degradation of the quality of the machined surface and gives a different surface roughness from the theoretical roughness. Indeed, this difference is significant, according to the cutting conditions used such as the cutting speed, the type of cutting tool, the workpiece material and the machining time. In addition, it should be noted here, as the wear is regular and does not exceed their tolerable value, the surface roughness (Ra) can increase gradually and the surface quality is acceptable [33].

The experimental results of the micrographs of the flank wear after several work sequences are shown in Fig. 11 according to the procedure recommended by the ISO 8688-1 standard. Observations of the damage on the cutting edge, for a cutting speed of 135 m/min, wear is observed and evolves at an accelerated rate and achieved the admissible

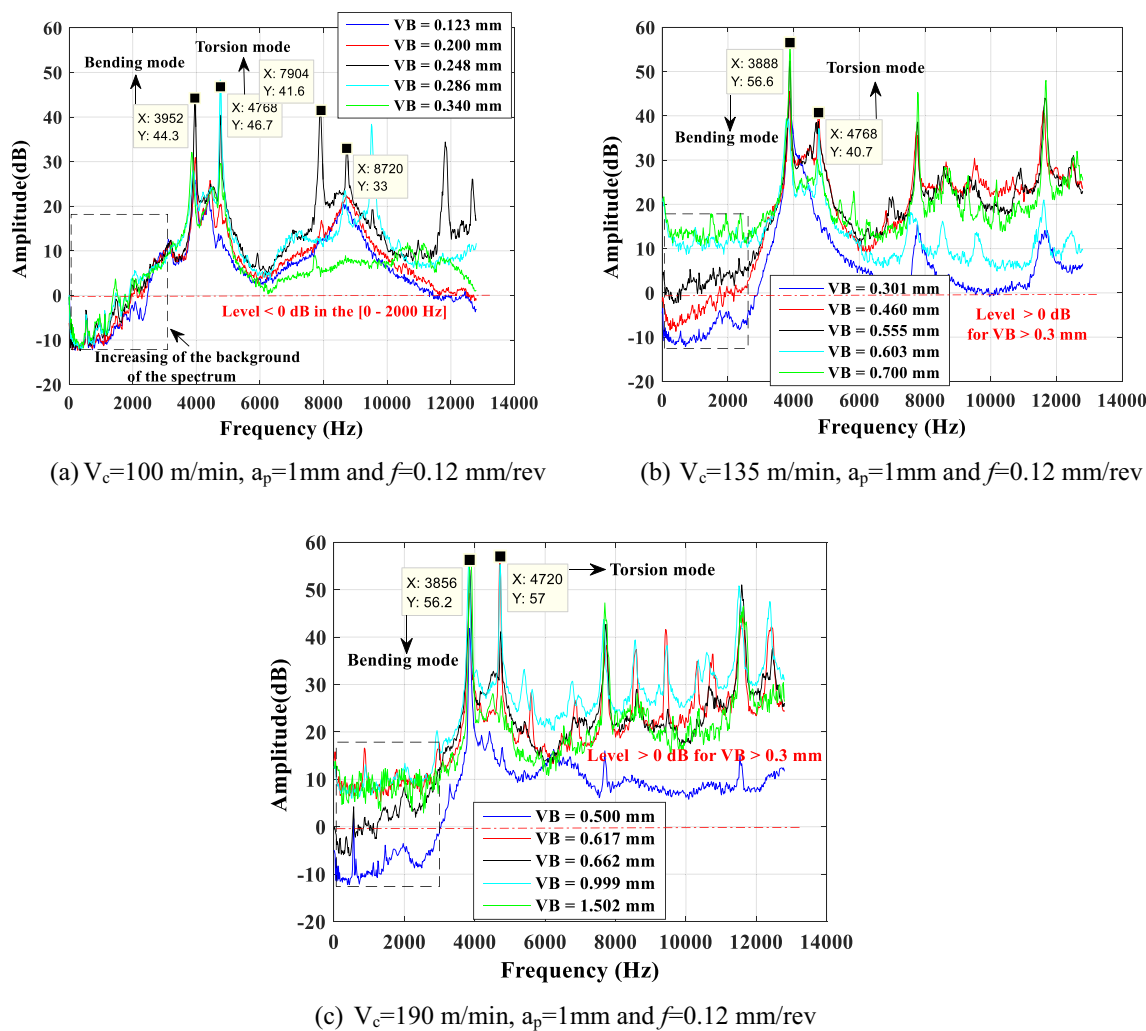


Fig. 10 The autospectra of the accelerations in the tangential direction for different sequences and with different flank wear (VB)

value $VB=0.5$ mm after 140 s. For the cutting speed 190 m/min, the mechanical and thermal stresses increase from one sequence to another and lead to rapid wear. When monitoring the mode of damage of the cutting tool with a depth of cut equal to 1 mm, it was noticed that its effect is less important than that of the cutting speed.

The evolution of wear morphology (flank wear and crater surfaces) over the entire machining time deserves special attention as it affects the surface finishing and dimensional accuracy of the workpiece. In this context, the analysis of the wear results shows that the influence of the cutting speed is significant. Machining during these cutting conditions becomes unstable, accompanied by increased vibration, which makes subsequent machining almost impossible.

Prediction of the Tool Lifespan

To determine reliable indicators that can give the correct decision regarding wear transitions, processing the obtained signals and spectra can help to monitor the transition of wear from the normal phase to the catastrophic phase. As soon as the onset of this last phase, the machining becomes difficult and therefore, the surface finish becomes poor and the precision will not meet the requirements of the definition drawing.

The temporal and frequency analysis of the cutting force signals will make it possible to extract a set of parameters likely to be considered subsequently as indicators of wear by looking for the relationship between these parameters and the development of flank wear. The monitoring process has been achieved as indicated previously in Fig. 4.

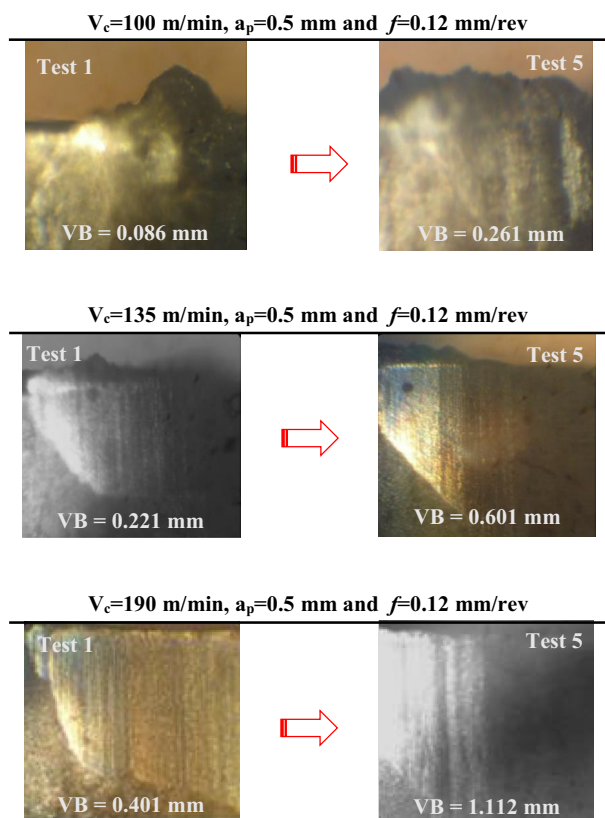


Fig. 11 Progression of flank wear (VB) after several work sequences

Frequency Analysis of Cutting Force Signals

Due to the acquisition limits of the dynamometer, the cutting forces are only measured in the frequency band (0–5.4) KHz. As the physical phenomena that occur at the tool-workpiece-machine interaction is complex, three-dimensional presentation of the signals and spectra of the cutting forces as a function of the flank wear VB is chosen.

The analysis of the signals and spectra (Fig. 12) in the radial direction, component most sensitive to wear [34], for three cutting speeds 100 m/min, 135 m/min and 190 m/min shows the main peaks that appear on the different spectra:

- A peak corresponding to the natural frequency of the platform in the x, y plane, which appears between 2800 and 3100 Hz. It is influenced by the rotation speed;
- A second peak appears between 3800 and 3900 Hz, corresponding to the first bending mode of the tool in its axial direction. In free vibration, this mode appears at 4000 Hz (Fig. 8a).

The analysis of the different spectra does not allow a clear appearance of tool wear, except a number of peaks that appear at low frequency between 1000 and 2000 Hz. The amplitudes of these peaks are very large compared to those

of the resonance frequency of the cutting tool. It is for this reason that the frequency axis starts from about 1000 Hz to reveal the natural frequency. Note that there is a significant increase in the amplitudes of the signals from one sequence to another with the increase in flank wear. The radial component of the cutting force shows the first natural frequency of the tool very clearly at about 4 kHz. In Fig. 12a where $V_c = 135$ m/min, it can be seen that the amplitude of the signal in the first sequence is very large. This may be due to the presence of the built-up edge, which causes an increase in the cutting force [33]. The wear appears very clearly for speeds 135 m/min and 190 m/min by the very significant increase in the amplitudes of the tool resonance frequency.

On the other hand, for the cutting speed 190 m/min, the mechanical and thermal stresses increase from one sequence to another and lead to rapid wear (VB and KT). In the fifth sequence, the development of wear leads to the collapse of the cutting tool edge, followed by a reduction in cutting forces due to the reduction in the depth of cut caused by the retreat of the cutting edge from the workpiece. The more we see a clear increase in the amplitude of the peak corresponding to the natural frequency of the tool with the increase in wear.

In this context, the analysis of the spectra does not allow a good follow-up of the wear evolution because the cutting force signals are very noisy. In the following section, the results obtained by the application of the Optimized Wavelet Multi-resolution Analysis (OWMRA) are presented. This efficacy tool can considerably improve the analysis using its denoising and filtering capacities. Mask effects (background noise and other components of the machine) can then be completely removed allowing to obtain more purified signals.

Spectral Analysis of Characteristic Frequencies by Optimized WMRA

For several cutting conditions, the profiles of the measured cutting force signals are very noisy. Using Optimized WMRA is like running these signals under a microscope, and waterfall filtering allows visualizing every part of the cutting force signal with adapted time and frequency resolution. The purpose of the analysis is to determine:

- The location of the changes as a function of time or position;
- The type of change: a break in the nose of the cutting tool, or a brusque change;
- The magnitude of the change in frequency peaks.

Figures 13, 14 and 15 show three examples of the radial cutting force (F_y) signals processed by the Optimized WMRA. As mentioned before, WMRA decomposes the

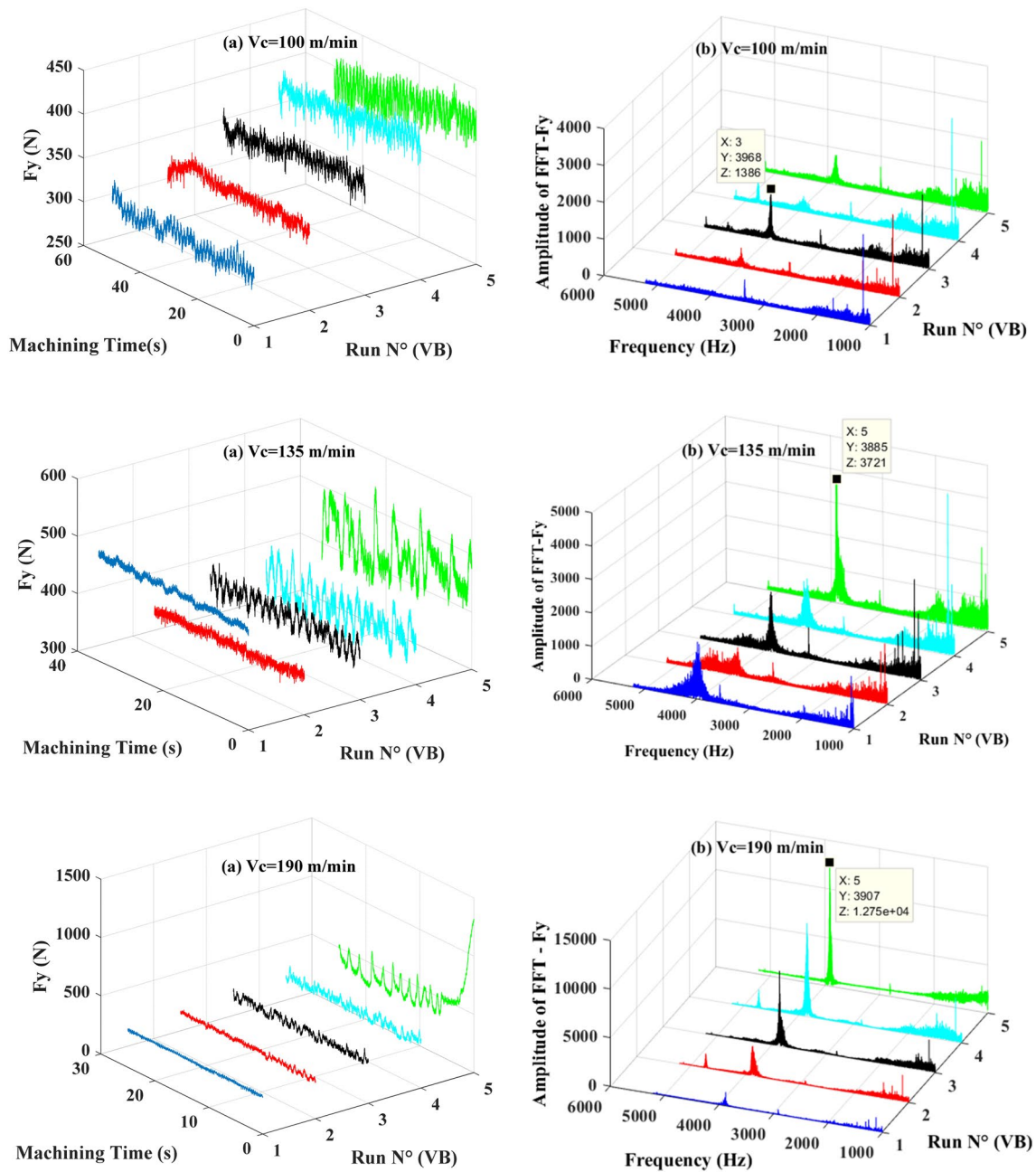


Fig. 12 **a** Variation of radial cutting force signals (F_y) and **b** the corresponding spectra according to VB

signal into several sub-signals with different frequency bands ranging from high to low frequencies. As the tool's wear occurs around the tool's natural frequency, so at high frequency range, the D1 (detail 1) component is taken as reconstructed signal since it is considered as high frequency narrow-band filtered signal. The other components correspond to low frequency range and do not have significant contribution on the tool's wear localization. For the cutting speed 100 m/min (Fig. 13) where VB is equal to 0.340 mm, a regular evolution of the cutting force as a

function of machining time is observed. The evolution of the reconstructed signal of detail D1 after filtering remains very regular. In this case, the machining is almost stable; no instability zone appears in the signal. Whereas for the cutting speed 135 m/min (Fig. 14) where VB is equal to 0.700 mm, certain areas of machining instability and disturbances in the time interval (9–35) s begin to appear. Finally, the machining becomes practically unstable for the speed 190 m/min (Fig. 15) because very high vibrations accompany it in the time interval (5–25) s. In this case,

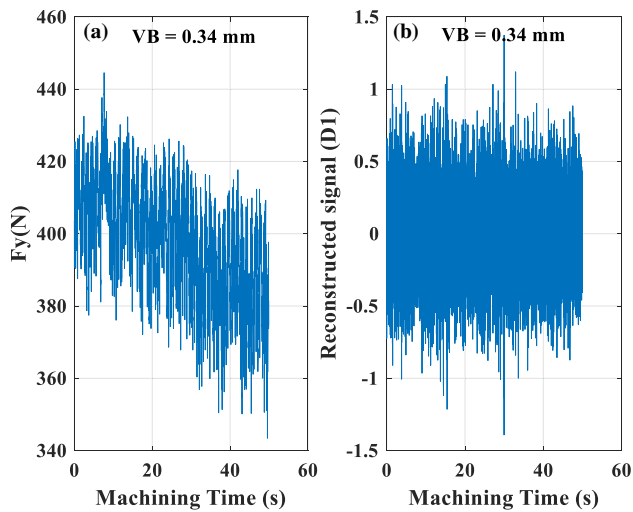


Fig. 13 **a** Variation of radial cutting force signals (F_y) and **b** reconstructed signal extracted from detail 1 for $V_c=100$ m/min, $a_p=1$ mm and $f=0.12$ mm/rev

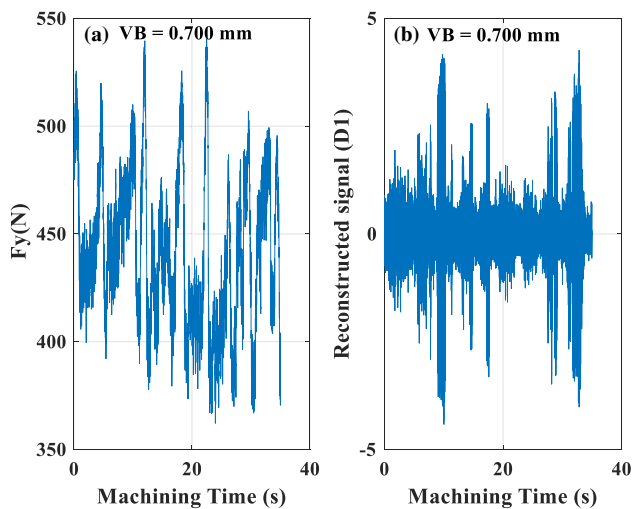


Fig. 14 **a** Variation of radial cutting force signals (F_y) and **b** reconstructed signal extracted from detail 1 for $V_c=135$ m/min, $a_p=1$ mm and $f=0.12$ mm/rev

machining is almost impossible and leads to catastrophic wear of the cutting tool edge with a flank wear equal to 1.502 mm.

The procedure of Envelope Analysis (EA) consists of three steps: load optimal reconstructed signal (D1) obtained after the application of the Optimized WMRA, then envelope extraction by the application of Hilbert Transform (HT) and the determination of the spectrum of the envelope by the application of the FFT [33]. The work method of envelope analysis is shown in Fig. 16.

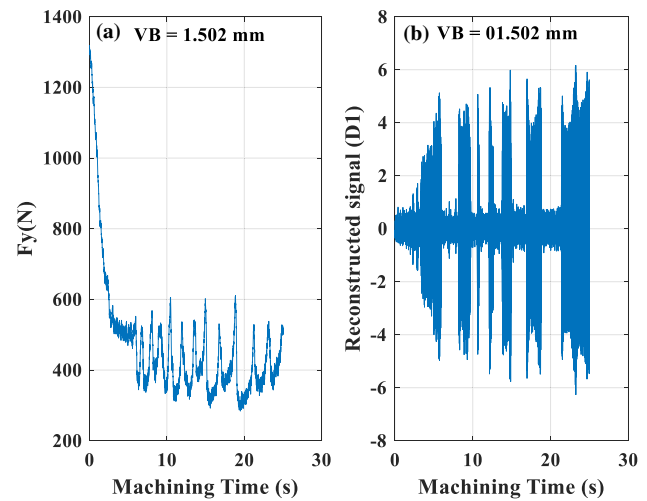


Fig. 15 **a** Variation of radial cutting force signals (F_y) and **b** reconstructed signal extracted from detail 1 for $V_c=190$ m/min, $a_p=1$ mm and $f=0.12$ mm/rev

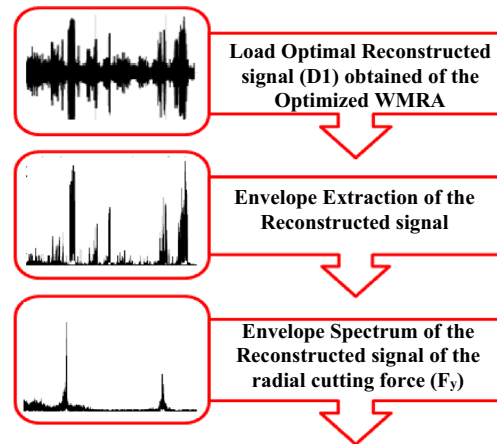


Fig. 16 Procedure of envelope analysis (EA)

Figure 17 shows the envelope spectra of the reconstructed signal (D1) obtained after the application of the waterfall algorithm of the OWMRA on cutting force signals. It enables the denoising of the signals and the disappearance of the resonance frequency of the cutting tool and the machining system. On the other hand, it shows two peaks, one in the frequency band (1–2) KHz and the second in the band (4.5–5) KHz in the case when flank wear of the cutting tool (VB) is greater than or equal to 0.3 mm.

The envelope spectrum of the radial component of the cutting force (F_y) for the cutting speed 100 m/min and a depth of cut 0.5 mm (Fig. 17a) does not show the two wear peaks because (VB) remains less than 0.3 mm, see Table 1. However, for the cutting speed $V_c=135$ m/min, two peaks are located from the third sequence where $VB \geq 0.3$ mm

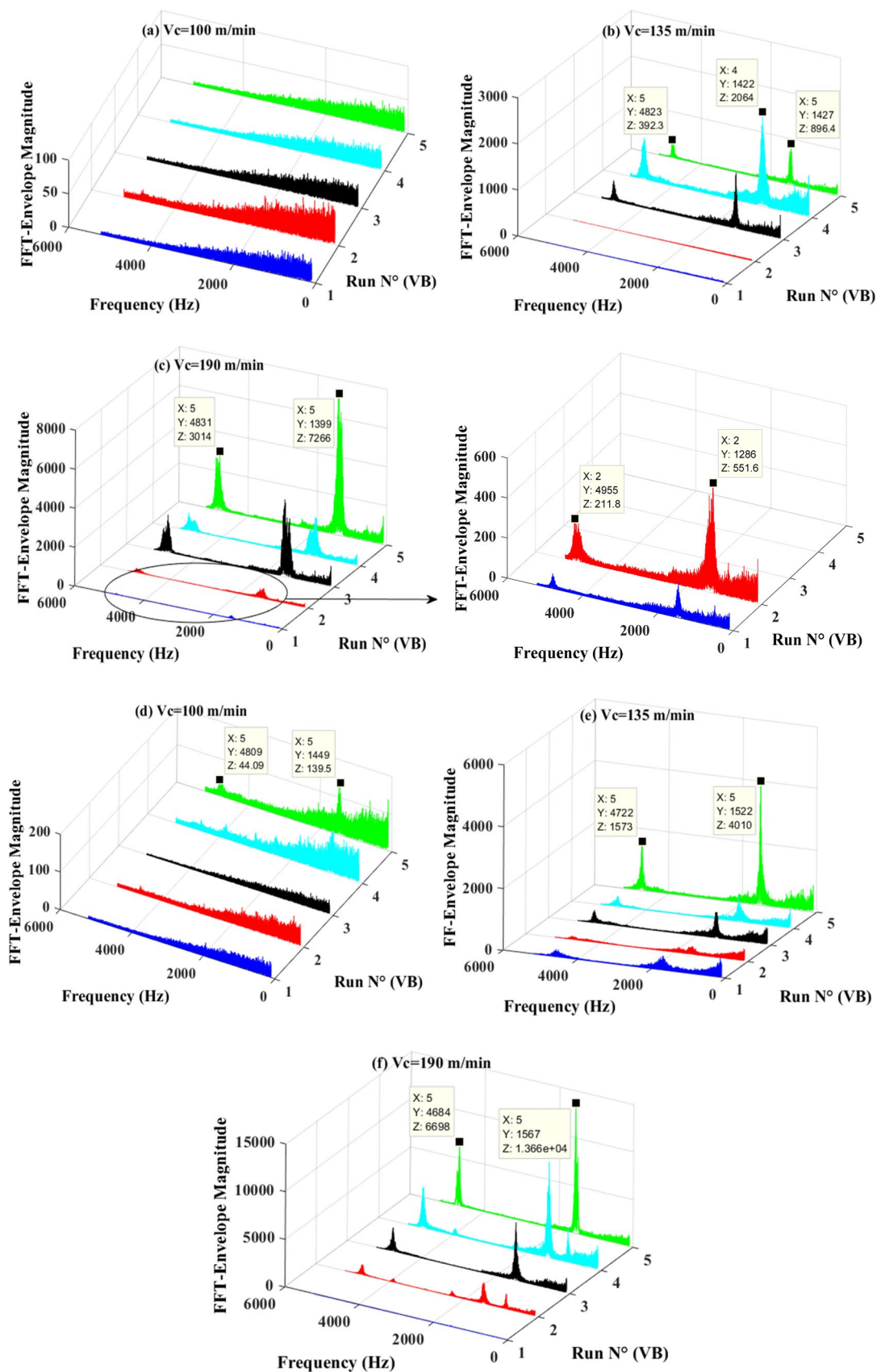


Fig. 17 Envelope spectra of the reconstructed signal (DI) according to VB

and do not appear in the first two sequences since the flank wear is lower than 0.3 mm. Moreover, there is a decrease in the amplitude of these two peaks in the fifth sequence (Fig. 17b). This is explained by the breakage of the nose of the cutting tool (retraction of the cutting edge compared to the machined workpiece) or VB is greater than 0.6 mm. Contrariwise, for the cutting speed 190 m/min (Fig. 17c), it can be noted the very clear appearance of the two wear peaks from the first sequence where VB is greater than 0.3 mm.

The increased cutting speed and depth of cut (a_p) cause a more rapid development of the flank wear. To this end, it is observed that the level of the amplitudes of the peaks increases several times with the increase in the cutting speed, especially from 135 m/min to 190 m/min. For the cutting speed 135 m/min (Fig. 17e), the two peaks can be seen very clearly with very high amplitudes in the fifth sequence. The increase in the cutting speed to 190 m/min (Fig. 17f) causes the appearance of several peaks on the different components, the phenomenon of chattering is established; the machining in this case becomes unstable.

The global analysis of these results shows that the optimized WMRA allowed the filtering and denoising of the cutting forces signals and reveals two peaks, which appear one below and the other above the resonance frequency of the cutting tool. Indeed, the characterization of the evolution of this spectrum level as a function of flank wear (VB) from the first test to the end of the tool lifespan; depends directly on the first frequency band [1500–2500 Hz]; which describes the natural frequencies of the Kistler platform and on the specific frequency band [4000–5500 Hz] and these are detected by the amplitude variation of the cutting force signals at these specific frequencies. In this context, these obtained results may well inform about the evolution of the wear of the cutting tool and can be considered as a good frequency indicator the prediction of the tool lifespan transition.

Proposed New Spectrum Indicator (OL_{mod}) for Prediction of the Tool Lifespan

Some previous studies ([11, 20, 21] and [24]) are examined the wear evolution and the tool breaking time with different methods and using a strategy based on five successive phases. First, the monitoring signal nature, the signal processing method, the data pre-processing method, the feature extraction, and finally the tool lifespan prediction method. A review of the recent published techniques shows specific contributions in monitoring wear and tool life prediction.

To take an over view of the behavior of the cutting forces according to the time, five signals measured during machining are concatenated as described in detail in Table 1. The idea is to see the general appearance of the normal wear

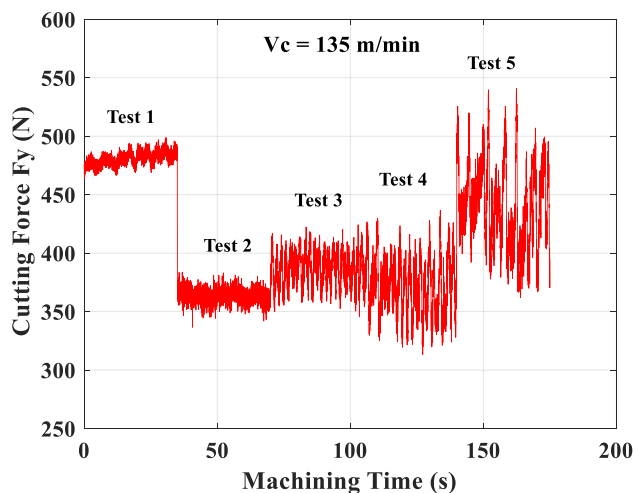


Fig. 18 Concatenation of measured signals of the cutting tool

period and then the transition to the catastrophic wear by applying the OL_{mod} indicator. Figure 18 shows by way of example, a concatenation of the five cutting force signals over the lifespan of the cutting tool for a speed of 135 m/min.

We wanted to find a wear indicator very easy to use in a monitoring system. For that, we proposed to use the frequency indicator called modified Overall Level (OL_{mod}) associated with the cutting force signals acquired during the lifespan of the cutting tool in the radial direction Y. The evaluation of this frequency indicator was performed by scanning the radial cutting force signals (F_y) using a sliding window of 1024 samples. In this context, as we said in the section before, we propose to initiate a slight modification on this frequency indicator around the resonant frequency of the cutting tool, delimited by F_{max} and F_{min} frequencies. The evolution of the vibration amplitudes of the natural frequencies of the cutting tool as a function of its degradation has proved that the band containing these frequencies 4000 Hz and 5500 Hz are the best qualified to follow its state and therefore identify wear and prediction of lifespan transition of the cutting tool.

Figures 19a, 20, 21a represent trends in the overall level OL_{mod} calculated from the concatenated cutting force signals over the lifespan of the cutting tool. It is clear that the application of this indicator is not effective in identifying the transition to the accelerated wear phase. Figures 19b, 20, 21b represent trends in the overall level OL_{mod} calculated from the concatenated reconstructed signals (D1) of the cutting forces over the lifespan of the cutting tool. In the Fig. 19b, the OL_{mod} has a slightly variable tendency around 2.5 as long as the wear VB value is still less than 0.5 mm. However, the OL_{mod} has an average value less

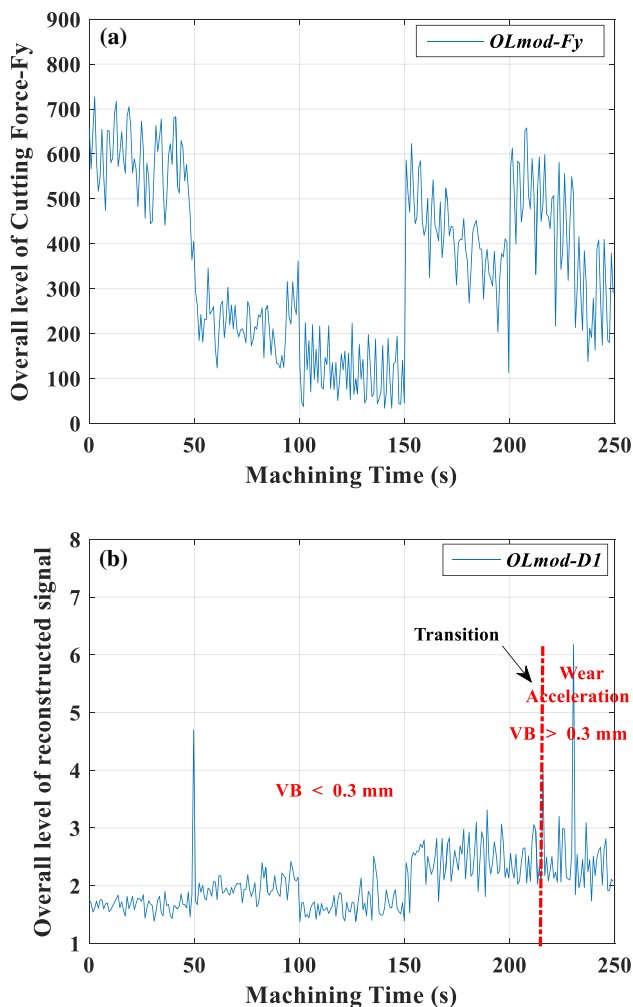


Fig. 19 Trend of the overall level (OL_{mod}) of cutting force and reconstructed signals over the entire cutting tool lifespan for $V=100$ m/min, $a_p=1$ mm and $f=0.12$ mm/rev

than 5 for a machining time of 105 s, corresponding to VB wear less than 0.555 mm. Above this time, the OL_{mod} increases slightly with the accelerated wear (Fig. 20b). In the last case (Fig. 21b), the OL_{mod} value remains less than 5 for a machining time of 30 s approximately, corresponding to VB wear less than 0.555 mm. Beyond this machining time, OL_{mod} increases significantly (Fig. 21b).

Based on these results, we propose an alarm criterion corresponding to exceeding the admissible wear of the cutting tool for OL_{mod} value equal to 5. Finally, it is obvious that the proposed frequency indicator provides effective monitoring of the transition of cutting tool lifespan to the accelerated wear.

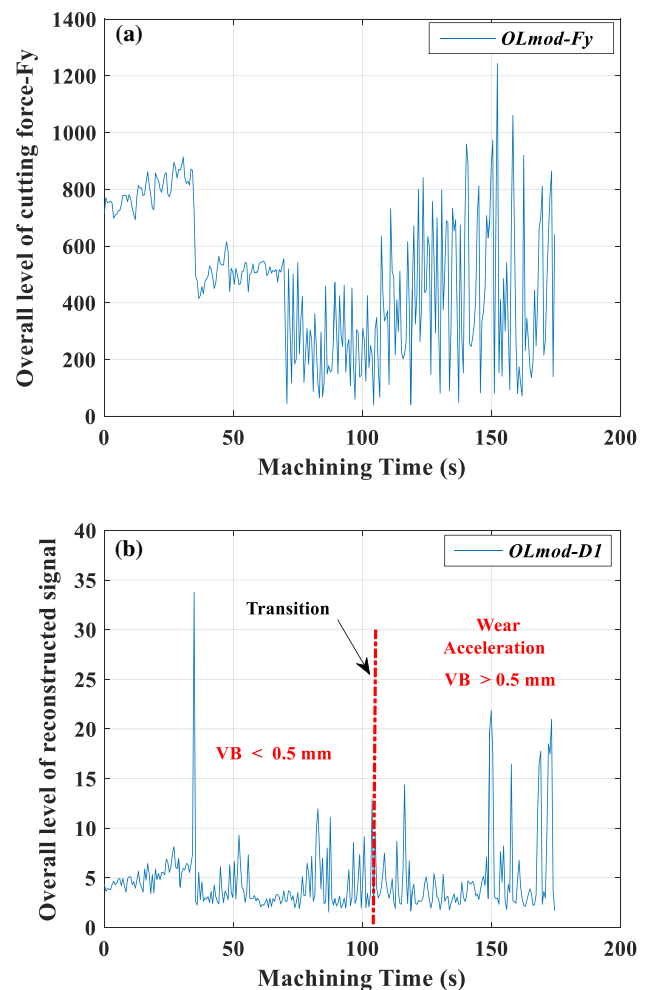


Fig. 20 Trend of the overall level (OL_{mod}) of cutting force and reconstructed signals over the entire cutting tool lifespan for $V=135$ m/min, $a_p=1$ mm and $f=0.12$ mm/rev

Conclusion

The work presented in this paper can be the basis for developing a real-time monitoring system for the evolution of cutting tool wear that can provide rapid alert when the allowable wear limit is exceeded during machining. The conclusions of this work that can be drawn are as follows:

- Monitoring tool wear from vibratory signals in both radial and tangential directions is possible based on the autospectra energy level. All the results obtained led to the determination of the changes in the state of the tool wear, which makes its evaluation possible.
- It was observed that the radial component of the cutting force is the most sensitive to the wear variation; this result is confirmed by the frequency analysis. The use of the Optimized Wavelet Multi-Resolution Analysis (OWMRA) enabled the denoising of the measured sig-

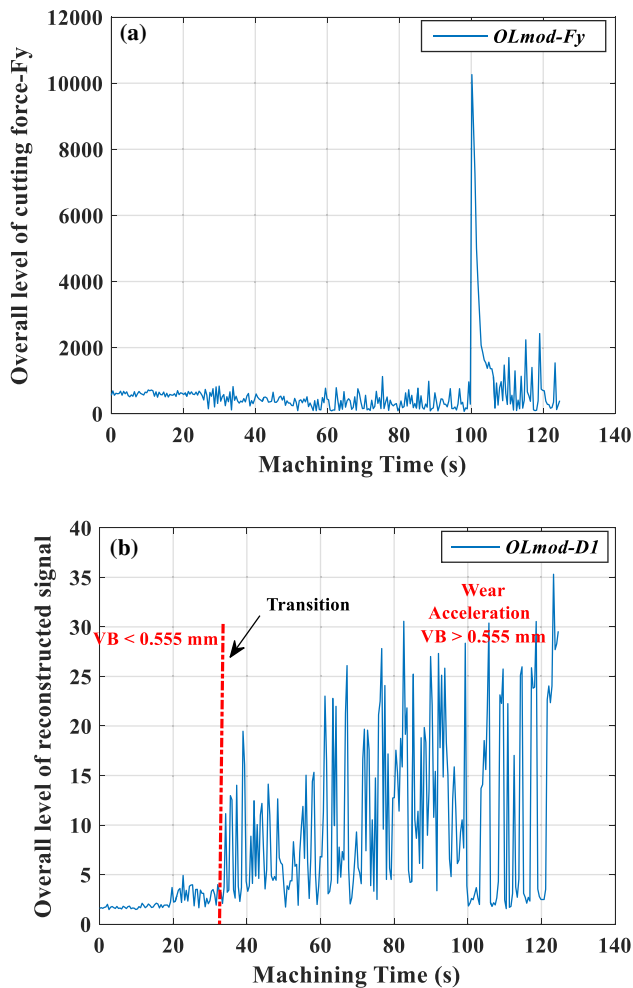


Fig. 21 Trend of the overall level (OL_{mod}) of cutting force and reconstructed signals over the entire cutting tool lifespan for $V=190$ m/min, $a_p=1$ mm and $f=0.12$ mm/rev

nals. The optimal reconstructed signal envelope spectrum highlights the appearance of two peaks below and above the natural frequency of the cutting tool directly related to the evolution of tool wear.

- The evolution of the amplitudes of the cutting tool natural frequencies as a function of its degradation through the modal test proved that the vibration energy is concentrated around the band [4000–5500] Hz, which is the best qualified to monitor wear and therefore predict the transition of cutting tool lifespan.
- The spectral indicator OL_{mod} , calculated from the cutting forces and reconstructed signals, has also shown its effectiveness of providing the moment of transition of the wear of its normal phase to accelerated phase around characteristic frequencies, corresponding to catastrophic wear leading to stopping machining at the appropriate time. This new indicator, once validated in offline tests, can be integrated into an online tool lifespan monitoring

system which can alert the user as soon as the transition criterion to catastrophic wear is reached.

The perspectives of this study, see the possibility of applying the best approach which can be integrated online in an expert system, with the aim of increasing industrial productivity; while ensuring the quality of machined surfaces and geometric tolerances required, which is a priority of advanced industry.

Acknowledgements The authors would like to thank the director and the engineer of Laboratory LMS, May 8th 1945 University of Guelma Algeria for their support and their help that they brought to our work. Additionally, we acknowledge financial support by the Algerian Ministry of Higher Education and Scientific Research.

Author Contributions Data acquisition and measurement setup were supplied by ON, BMK and DMC. Methodology, data processing and analysis: ON, BMK, ZO, DA and CL. Redaction: BMK and revision: DA. Supervision of the article: ON.

Funding This study was achieved out with the research resources of the Laboratory LMS, May 8th 1945 University of Guelma, Algeria. This work received financial support from the Algerian Ministry of Higher Education and Scientific Research and the Delegated Ministry for Scientific Research through PRFU research project: A11N01UN240120180003.

Declarations

Conflict of interest I, Doctor BABOURI Mohamed Khemissi, corresponding author of the paper: “Experimental investigation of tool lifespan evolution during turning operation based on the new spectral indicator OL_{mod} ”, submitted for publication to the Journal of Vibration Engineering & Technologies, certify that we have no potential conflict of interest for the mentioned article. Moreover, I certify that the paper follows the ethical rules of good scientific practice mentioned in the “Ethical Responsibilities of Authors” of the journal. Herewith, I confirm, on behalf of all authors, that the information provided is accurate.

References

1. Kuntoğlu M, Salur E, Gupta MK, Sarıkaya M, Pimenov DY (2021) A state-of-the-art review on sensors and signal processing systems in mechanical machining processes. *Int J Adv Manuf Technol* 116(9):2711–2735
2. Zhou Y, Xue W (2018) Review of tool condition monitoring methods in milling processes. *Int J Adv Manuf Technol* 96(5):2509–2523
3. Kuntoğlu M, Sağlam H (2021) Investigation of signal behaviors for sensor fusion with tool condition monitoring system in turning. *Measurement* 173:108582. <https://doi.org/10.1016/j.measurement.2020.108582>
4. Zhou JM, Andersson M, Ståhl JE (1995) A system for monitoring cutting tool spontaneous failure based on stress estimation. *J Mater Process Technol* 48(1–4):231–237
5. Li X, Dong S, Yuan Z (1999) Discrete wavelet transform for tool breakage monitoring. *Int J Mach Tools Manuf* 39(12):1935–1944

6. Oo H, Wang W, Liu Z (2020) Tool wear monitoring system in belt grinding based on image-processing techniques. *Int J Adv Manuf Technol* 111(7):2215–2229
7. Zhou C, Yang B, Guo K, Liu J, Sun J, Song G, Zhu S, Sun C, Jiang Z (2020) Vibration singularity analysis for milling tool condition monitoring. *Int J Mech Scie* 166:105254
8. Navarro-Devia JH, Dao DV, Chen Y, Li H (2021) Analysis of Vibration Signals in Monitoring Titanium End Milling Process Using Triaxial Accelerometer. In *Int Manuf Science and Engineering Conference*. ASME, 85062, p. V001T05A018
9. Huang PL, Li JF, Sun J, Jia XM (2016) Cutting signals analysis in milling titanium alloy thin-part components and non-thin-wall components. *Int J Adv Manuf Technol* 84(9):2461–2469
10. Bouchareb A, Lagred A, Amirat A (2019) Effect of the interaction between depth of cut and height-to-width ratio of a workpiece on vibration amplitude during face milling of C45 steel. *Int J Adv Manuf Technol* 104(1):1221–1227
11. Chiou RY, Liang SY (2000) Analysis of acoustic emission in chatter vibration with tool wear effect in turning. *Int J Mach Tools Manuf* 40(7):927–941
12. Zhu K, Zhang Y (2019) A generic tool wear model and its application to force modeling and wear monitoring in high speed milling. *Mech Syst Signal Process* 115:147–161
13. Hui Y, Mei X, Jiang G, Tao T, Pei C, Ma Z (2019) Milling tool wear state recognition by vibration signal using a stacked generalization ensemble model. *Shock Vib* 2019:7386516–7386523. <https://doi.org/10.1155/2019/7386523>
14. Arslan H, Er A, Orhan S, Aslan E (2016) Tool condition monitoring in turning using statistical parameters of vibration signal. *Int J of Acoust Vibrations* 21(4):371–378
15. Bombiński S, Kossakowska J, Jemielniak K (2022) Detection of accelerated tool wear in turning. *Mech Syst Signal Process* 162:108021. <https://doi.org/10.1016/j.ymssp.2021.108021>
16. Prasad BS, Babu MP (2017) Correlation between vibration amplitude and tool wear in turning: numerical and experimental analysis. *Eng Sci Technol Int J* 20(1):197–211
17. Babouri MK, Ouelaa N, Djamaa MC, Djebala A, Boucherit S, Hamzaoui N (2019) Prediction of optimal lifetime of the tool's wear in turning operation of AISI D3 steel based on the new spectral indicator SCG. *Comput Methods Exp Testing Mech Eng*. https://doi.org/10.1007/978-3-030-11827-3_9
18. Babouri MK, Ouelaa N, Djebala A (2014) Temporal and frequential analysis of the tools wear evolution. *Mechanics* 20(2):205–212
19. Yuan J, Li J, Wei W, Liu P (2022) Operational modal identification of ultra-precision fly-cutting machine tools based on least-squares complex frequency-domain method. *Int J Adv Manuf Technol* 119:4385–4394
20. Nouioua M, Bouhalais ML (2021) Vibration-based tool wear monitoring using artificial neural networks fed by spectral centroid indicator and RMS of CEEMDAN modes. *Int J Adv Manuf Technol* 115(9):3149–3161
21. Babouri MK, Ouelaa N, Djebala A (2016) Experimental study of tool life transition and wear monitoring in turning operation using a hybrid method based on wavelet multi-resolution analysis and empirical mode decomposition. *Int J Adv Manuf Technol* 82:2017–2028
22. Babouri MK, Ouelaa N, Djebala A (2017) Application of the empirical mode decomposition method for the prediction of the tool wear in turning operation. *Mechanics* 23(2):315–320
23. Xu C, Chai Y, Li H, Shi Z (2018) Estimation the wear state of milling tools using a combined ensemble empirical mode decomposition and support vector machine method. *J Adv Mech Design Syst Manuf* 12(2):JAMDSM0059–JAMDSM0059
24. Bouhalais ML, Nouioua M (2021) The analysis of tool vibration signals by spectral kurtosis and ICEEMDAN modes energy for insert wear monitoring in turning operation. *Int J Adv Manuf Technol* 115(9):2989–3001
25. Babouri MK, Ouelaa N (2018) Analyse vibratoire de l'usure des outils de coupe : Surveillance de l'évolution de l'usure d'un outil de coupe en tournage. Éditions universitaires européennes
26. Mallat SG (1989) A theory for multiresolution signal decomposition: the wavelet representation. *IEEE Trans Pattern Anal Mach Intell* 11(7):674–693
27. Djebala A, Ouelaa N, Benchaabane C, Laefer DF (2012) Application of the wavelet multi-resolution analysis and Hilbert transform for the prediction of gear tooth defects. *Meccanica* 47:1601–1612
28. Djebala A, Babouri MK, Ouelaa N (2015) Rolling bearing fault detection using a hybrid method based on empirical mode decomposition and optimized wavelet multi-resolution analysis. *Int J Adv Manuf Technol* 79:2093–2105
29. Yang Q, Wang B, Deng J, Zheng Y, Kong X (2022) The effect of addition of MWCNT nanoparticles to CryoMQL conditions on tool wear patterns, tool life, roughness, and temperature in turning of Ti-6Al-4 V. *Int J Adv Manuf Technol*. <https://doi.org/10.1007/s00170-022-09101-7>
30. Bouzid L, Yallese MA, Belhadi S, Boulanouar L (2017) Tool Life Evaluation of Cutting Materials in Turning of X20Cr13 Stainless Steel. In *Applied Mechanics, Behavior of Materials, and Engineering Systems, Lecture Notes in Mechanical Engineering*. Springer, Cham, pp. 447–452. https://doi.org/10.1007/978-3-319-41468-3_37
31. Babouri MK, Ouelaa N, Djamaa MC, Djebala A, Hamzaoui N (2017) Prediction of tool wear in the turning process using the spectral center of gravity. *J Fail Anal Prev* 17(5):905–913
32. Sandvik Coromant, Outils de coupe Sandvik Coromant, Tournage-Fraisage-Perçage-Alésage-Attachements (2009)
33. Yallese MA (2005) Etude du comportement à l'usure des matériaux de coupe modernes en tournage dur. Thesis University of Badji Mokhtar Annaba, Algeria
34. Feldman M (2011) Hilbert transform in vibration analysis. *Mech Syst Signal Process* 25:735–802

Publisher's Note Springer Nature remains neutral with regard to jurisdictional claims in published maps and institutional affiliations.

Springer Nature or its licensor (e.g. a society or other partner) holds exclusive rights to this article under a publishing agreement with the author(s) or other rightsholder(s); author self-archiving of the accepted manuscript version of this article is solely governed by the terms of such publishing agreement and applicable law.